RINMANITE, Zn₂Sb₂Mg₂Fe₄O₁₄(OH)₂, A NEW MINERAL SPECIES WITH A NOLANITE-TYPE STRUCTURE FROM THE GARPENBERG NORRA MINE, DALARNA, SWEDEN

DAN HOLTSTAM[§]

Department of Mineralogy, Research Division, Swedish Museum of Natural History, Box 50007, SE–104 05 Stockholm, Sweden

KJELL GATEDAL

School of Mines and Metallurgy, Box 173, SE–682 24 Filipstad, Sweden

KARIN SÖDERBERG AND ROLF NORRESTAM

Department of Structural Chemistry, Arrhenius Laboratory, Stockholm University, SE–106 91 Stockholm, Sweden

ABSTRACT

Rinmanite, ideally $Zn_2Sb_2Mg_2Fe_4O_{14}(OH)_2$, is a new mineral species from the Garpenberg Norra Zn–Pb mine, Hedemora, Dalarna, in south-central Sweden, where it occurs in a skarn assemblage associated with tremolite, manganocummingtonite, talc, franklinite, barite and svabite. Rinmanite crystals are prismatic, up to 0.5 mm in length, with good {100} cleavage. The VHN_{100} is in the range 841–907. $D_{calc} = 5.13(1)$ g•cm⁻³. The mineral is black (translucent dark red in thin splinters) with a submetallic luster. The mineral is moderately anisotropic and optically uniaxial (–). Reflectance values measured in air are 13.5–12.1% (λ = 470 nm), 12.9–11.8% (546 nm), 12.6–11.7% (589 nm) and 12.2–11.3% (650 nm). Electron-microprobe analyses of rinmanite (wt.%) gave MgO 8.97, Al_2O_3 0.82, MnO 2.47, Fe_2O_3 34.33, ZnO 14.24, Sb_2O_5 36.31, H_2O 1.99 (calculated), sum 99.13, yielding the empirical formula $(Zn_{1.58}Mn_{0.31}Mg_{0.06})_{\Sigma1.95}Sb_{2.03}[Mg_{1.95}Fe_{3.88}Al_{0.15}]_{\Sigma5.98}O_{14.01}(OH)_{1.99}$. Rinmanite is hexagonal, space group $P6_3mc$, with a 5.9889(4), c 9.353(1) Å, V 290.53(5) Å³ and $Z = 1$. A structure refinement from single-crystal MoKα X-ray-diffraction data ($R = 3.1\%$ for 199 reflections) shows that rinmanite is isostructural with nolanite. The octahedral $M(1)$ and $M(2)$ sites are occupied by (Mg + Fe) and Sb, respectively, whereas Zn is located at the 4-coordinated $M(3)$ site. The strongest eight lines in the powder-diffraction pattern [d in Å (I_{obs})(*hkl*)] are: 5.19(20)(100), 3.47(34)(102), 2.99(43)(110), 2.67(44)(103), 2.522(100)(112), 1.660(28)(213), 1.517(33)(205) and 1.497(54)(220). Mössbauer spectroscopy confirms that rinmanite contains Fe^{3+} at octahedral sites and is in a paramagnetic state down to at least 77 K. Rinmanite is believed to have formed during prograde metamorphism of an initially low-S, siliceous carbonate protolith enriched in Zn, Sb and Fe, at relatively high $P(H_2O)$. The new mineral species is named after Sven Rinman (1720–1792), of *Bergskollegium*.

Keywords: rinmanite, new mineral species, crystal structure, nolanite, skarn, Garpenberg Norra, Sweden.

SOMMAIRE

La rinmanite, dont la composition idéale est $Zn_2Sb_2Mg_2Fe_4O_{14}(OH)_2$, est une nouvelle espèce minérale découverte à la mine de Zn–Pb de Garpenberg Norra, Hedemora, Dalarna, dans la partie centre-sud de la Suède, dans un assemblage de skarn en association avec trémolite, manganocummingtonite, talc, franklinite, barite et svabite. Les cristaux de rinmanite sont prismatiques, atteignant jusqu'à 0.5 mm en longueur, avec un bon clivage {100}. La dureté VHN_{100} est dans l'intervalle 841–907. $D_{calc} =$ 5.13(1) g•cm⁻³. C'est un minéral noir, mais translucide rouge foncé dans les écailles, avec un éclat submétallique. La rinmanite est moyennement anisotrope et optiquement uniaxe (–). Les mesures de réflectance ont été faites dans l'air: 13.5–12.1% (λ = 470 nm), 12.9–11.8% (546 nm), 12.6–11.7% (589 nm) et 12.2–11.3% (650 nm). Les analyses à la microsonde électronique ont donné, en poncentages pondéraux: MgO 8.97, Al_2O_3 0.82, MnO 2.47, Fe_2O_3 34.33, ZnO 14.24, Sb_2O_5 36.31, H_2O 1.99 (calculé), somme 99.13, menant à la formule empirique $(Zn_{1.58}Mn_{0.31}Mg_{0.06})_{\Sigma1.95}Sb_{2.03}[Mg_{1.95}Fe_{3.88}Al_{0.15}]_{\Sigma5.98}O_{14.01}(OH)_{1.99}$. La rinmanite est hexagonale, groupe spatial $P6_3mc$, avec a 5.9889(4), c 9.353(1) Å, V 290.53(5) Å³ et $Z = 1$. Un affinement de la structure, utilisant des données en diffraction X obtenues sur cristal unique (rayonnement MoKα), a atteint un résidu R de 3.1% pour 199 réflexions; la rinmanite est isostructurale de la nolanite. Les sites octaédriques $M(1)$ et $M(2)$ sont attribués à (Mg + Fe) et Sb, respectivement, tandis que le Zn se trouve dans le site $M(3)$, à coordinence tétraédrique. Les huit raies les plus intenses du spectre de diffraction, méthode des poudres [d en Å (I_{obs})(*hkl*)] sont: 5.19(20)(100), 3.47(34)(102), 2.99(43)(110), 2.67(44)(103), 2.522(100)(112),

§ *E-mail address*: dan.holtstam@nrm.se

1.660(28)(213), 1.517(33)(205) et 1.497(54)(220). La spectroscopie de Mössbauer confirme que la rinmanite contient le Fe^{3+} aux sites octaédriques et se trouve dans un état paramagnétique jusqu'à au moins 77 K. La rinmanite se serait formée au cours d'un métamorphisme prograde d'un protolithe siliceux et carbonaté, à faible teneur en soufre mais enrichi en Zn, Sb et Fe, à $P(H_2O)$ relativement élevé. La nouvelle espèce honore Sven Rinman (1720–1792), du *Bergskollegium*.

(Traduit par la Rédaction)

Mots-clés: rinmanite, nouvelle espèce minérale, structure cristalline, nolanite, skarn, Garpenberg Norra, Suède.

INTRODUCTION

During an extensive petrographic study of silicate skarns from the Garpenberg Norra mine in south-central Sweden, an exotic assemblage of minerals consisting mainly of amphibole first attracted our attention owing to the presence of an unusual reddish mineral. The assemblage was subsequently shown to contain a hitherto unknown Zn–Sb–Mg–Fe–H oxymineral. Our purpose here is to formally announce this new mineral species and to put forward some hypotheses on its formation.

The name of the new mineral species honors the memory of Sven Rinman (1720–1792), a mining scientist, metallurgist and chemist who was a member of *Bergskollegium* (the Board of Mines). He is sometimes considered the father of the Swedish mineral industry. Holotype material, including a polished mount on which most of the characterization was done, is preserved at the Department of Mineralogy, Swedish Museum of Natural History, where it is registered as #2000160. The mineral and its name were approved by the IMA Commission on New Minerals and Mineral Names prior to publication.

OCCURRENCE

The Garpenberg Norra mine in Hedemora, Dalarna (= Dalecarlia), Sweden, is situated in the Garpenberg ore district, where mines have been worked for base metals for at least 700 years, and still are a major source in northern Europe. The Garpenberg Norra deposit consists of Zn–Pb–Fe–Cu–Sb–Ag-mineralized supracrustal units (marble + altered felsic volcaniclastic rocks). The sulfide ores, dominated by sphalerite, galena and pyrite, form lenses and veinlets in close association with dolomite marble and silicate skarns (Sandecki 1983). Geological and geochemical lines of evidence indicate that the ores of the district represent tectonically deformed and metamorphosed equivalents to stratabound volcanic-exhalative massive sulfide deposits (Vivallo 1985). In addition, detailed facies-analysis of the host rocks suggests that the sulfide mineralization largely resulted from synvolcanic replacements below the seafloor (Allen *et al.* 1996). The peak conditions of metamorphism of the area, prevailing in conjunction with the Svecofennian orogeny at *ca* 1.85 Ga, are estimated to be $T \geq 550°C$ and $P \leq 3.5$ kbar (Vivallo 1984).

The investigated sample, *ca.* $50 \times 30 \times 20$ mm in size, was collected from a skarn enclave within dolomite marble at the 990-m level in the mine. It is dominated by a reddish orange amphibole-rich assemblage, with individual crystal fibers up to 10 mm in length, in contact with granular dolomite and calcite (Fig. 1). The dominant species is Mn-bearing tremolite, which commonly contains patchy inclusions and overgrowths of zincian manganocummingtonite. The latter mineral is suspected to be responsible for a rather intense
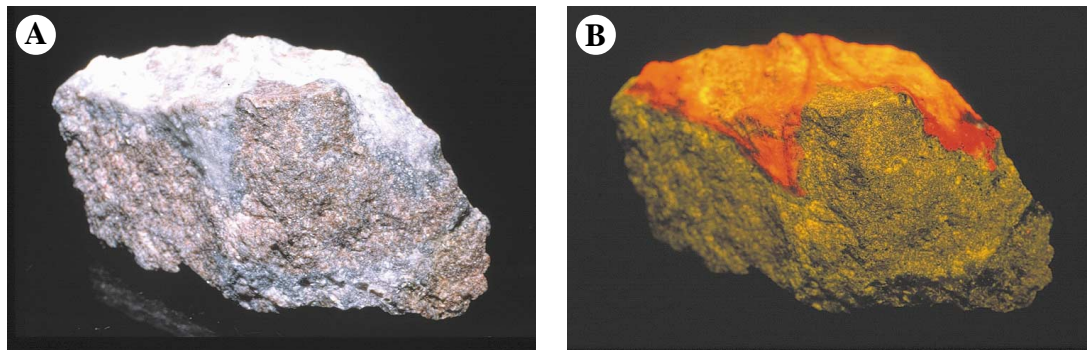

FIG. 1.   A. Specimen (*ca.* 5 cm wide) with carbonates (white), amphibole (reddish) and franklinite–rinmanite (dark spots). B. Same specimen illuminated with UV light (254 nm).

yellow-orange response of the assemblage in ultraviolet light at a wavelength of 254 nm. The amphiboles are intimately associated with minor amounts of manganoan talc. Irregular black clusters in the rock consist mainly of franklinite and rinmanite. Microscopic amounts of barite and svabite, $Ca_5(AsO_4)_3F$, also have been detected. Rinmanite occurs both as isolated crystals within the silicate matrix (commonly adjacent to talc) and in aggregates lining franklinite (Fig. 2).

Physical and optical properties

Rinmanite is black and opaque with a submetallic luster (dark red translucent in thin splinters). The streak is brown. The density was not determined experimentally, but a calculated value of 5.13(1) g•cm^{-3} is based on the unit-cell contents. Vickers Hardness Numbers were obtained using a Shimadzu type-M microhardness tester loaded with a 100 g weight. The indentations were nearly straight and accompanied by few radial fractures. The average of five measurements is 880 (range 841–907), which corresponds to a Mohs hardness of about 6. The crystals are mostly euhedral and prismatic, elongate along [001], and their maximum dimension is *ca.* 0.5 mm. Penetration twins are common. Cleavage is well developed parallel to {100}, and the fracture is splintery. The cleavage traces give rise to vertical striations on the crystals.

Reflectance measurements have been made within the visible spectrum, using a Zeiss MPM800 photometer system, equipped with a 10×/0.20 Ultrafluar

objective, and adjusted to give a field of measurement with a diameter of 30 μm. The step size (equal to bandwidth) was 20 nm, and SiC (Zeiss no. 846) was used as a standard. Reflectance values from a maximum-bireflectance grain are tabulated in Table 1. The results conform to a microscope observation of rinmanite in reflected, polarized light, *i.e.*, the mineral is grey, lacks visible dichroism, and is weakly bireflectant. Under crossed polars, it is moderately anisotropic. Its reflectance properties are very different from those of nolanite (Fig. 3), with which it is isostructural (see below). If the data are compared with the >500 minerals listed in the *Quantitative Data File for Ore Minerals* (Criddle & Stanley 1993), the closest resemblance found, in terms of overall reflectance and dispersion, is with filipstadite (another rare oxymineral of Sb and Fe).

In transmitted light, rinmanite is uniaxial negative and dichroic, with *O* dark red and *E* orange-red. Ap-

TABLE 1. OPTICAL REFLECTANCE DATA (%)
FOR RINMANITE

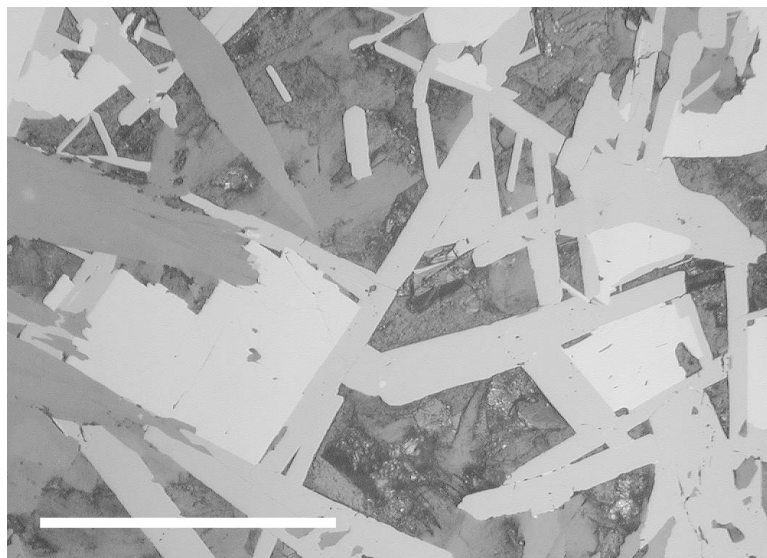| λ (nm)	R_O	R_E	λ (nm)	R_O	R_E
400	14.9	13.4	560	12.8	11.7
420	14.5	12.9	580	12.7	11.7
440	14.0	12.5	600	12.6	11.6
460	13.6	12.2	620	12.4	11.5
480	13.4	12.1	640	12.3	11.4
500	13.3	11.9	660	12.1	11.3
520	13.1	11.9	680	12.0	11.2
540	12.9	11.8	700	12.0	11.2

SiC standard in air.

FIG. 2.   Photomicrograph (reflected light) of a polished section of rinmanite and franklinite (white) with associated silicates. Length of white bar is 0.2 mm.

proximate indices of refraction, calculated from the reflectance data using the Fresnel equation, are $\omega = 2.10$ and $\varepsilon' = 2.04$ at $\lambda = 589$ nm. A Gladstone–Dale calculation gives a compatibility index of 0.032, which is considered excellent (Mandarino 1981).

CHEMICAL DATA

Elemental analysis

Chemical analyses of rinmanite were carried out with a Cameca SX50 electron microprobe operated at 20 kV and 15 nA, with a beam diameter of 1 μm. Stibnite (Sb$L\alpha$), ZnS (Zn$K\alpha$), Fe$_2$O$_3$ (Fe$K\alpha$), MnTiO$_3$ (Mn, Ti$K\alpha$), wollastonite (Ca$K\beta$), Al$_2$O$_3$ (Al$K\alpha$), MgO (Mg$K\alpha$) and albite (Na, Si$K\alpha$) were used as standards. The raw data were processed in the Cameca version of the PAP routine (Pouchou & Pichoir 1991). Back-scattered electron imaging indicated only slight chemical heterogeneity in the crystals; selected results from a data set of 30 point analyses in total are given in Table 2. Ca, Na and Si were found to be below the detection level in rinmanite. The average chemical formula (based on 16 O atoms) is $(Zn_{1.58}Mn_{0.31}Mg_{0.06})_{\Sigma 1.95}\ Sb_{2.03}[Mg_{1.95}Fe_{3.88}\ Al_{0.15}]_{\Sigma 5.98}O_{14.01}(OH)_{1.99}$ Analytical data for some associated minerals are reproduced in Table 3.

Mössbauer spectroscopy

Mössbauer spectra were obtained from a 3-mg powdered sample, run at magic-angle geometry (54.7°) at

room and liquid N$_2$ temperatures using a constant-acceleration Mössbauer spectrometer (Wissenschaftliche Elektronik GmbH) and stored in a 1024-channel analyzer. Velocity calibration was done using a 25-μm foil of α-Fe. Spectral analyses, assuming a thin absorber and a Lorentzian line shape, were carried out using the software developed by Jernberg & Sundqvist (1983). The centroid shift (CS), quadrupole splitting (QS) and line width (Γ) are parameters used to characterize the absorption doublet found (Fig. 4). The results (values in

TABLE 2. CHEMICAL COMPOSITION OF RINMANITE

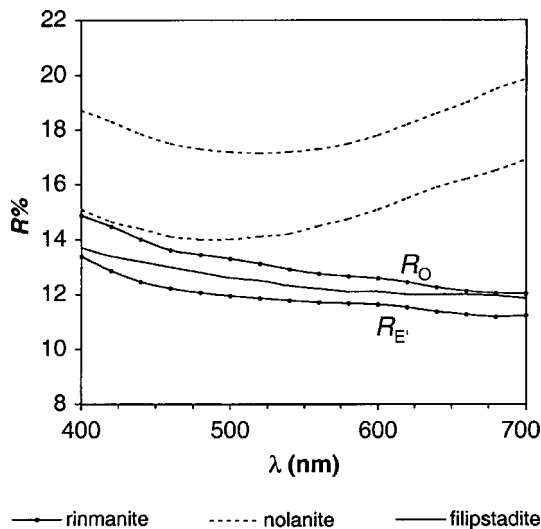| anal. no.	4	7	13	15	23	24	mean (n = 30)	std. dev. (n = 30)
				wt.% oxide				
MgO	8.73	9.24	8.65	9.32	9.38	8.55	8.97	0.24
Al$_2$O$_3$	0.63	0.84	0.99	0.79	0.94	0.68	0.82	0.09
TiO$_2$	0.00	0.01	0.02	0.00	0.02	0.00	0.01	0.01
MnO	2.31	2.43	2.48	2.45	2.44	2.45	2.47	0.08
Fe$_2$O$_3$	34.06	34.15	34.64	33.69	34.40	34.37	34.33	0.23
ZnO	14.59	13.80	14.13	14.04	14.00	14.76	14.24	0.26
Sb$_2$O$_5$	36.70	36.84	35.40	36.44	36.70	36.07	36.31	0.37
H$_2$O (calc)							1.99	
Total	97.02	97.31	96.30	96.72	97.88	96.88	99.13	
				10 metal atoms				
Mg	1.98	2.08	1.96	2.10	2.09	1.94	2.02	0.05
Al	0.11	0.15	0.18	0.14	0.16	0.12	0.15	0.02
Mn	0.30	0.31	0.32	0.31	0.31	0.32	0.32	0.01
Fe	3.90	3.87	3.96	3.83	3.86	3.93	3.90	0.03
Zn	1.64	1.53	1.58	1.57	1.54	1.66	1.59	0.03
Sb	2.07	2.06	2.00	2.05	2.03	2.04	2.04	0.02
H							2.00	

FIG. 3. Reflectance spectra for rinmanite (line with dots), nolanite (dashes and dots) and filipstadite (full line). The data for nolanite and filipstadite are taken from Criddle & Stanley (1993).

TABLE 3. SELECTED ANALYTICAL DATA FOR MINERALS ASSOCIATED WITH RINMANITE

anal. no.	manganocummingtonite A1	A2	tremolite A3	A4	franklinite B1	B2
			wt.% oxide			
SiO$_2$	58.43	58.05	59.52	58.22	0.07	0.00
TiO$_2$	0.00	0.00	0.00	0.00	0.01	0.04
Al$_2$O$_3$	0.05	0.00	0.14	0.16	0.97	0.74
Fe$_2$O$_3$	0.27	0.26	0.07	0.11	66.33	66.45
ZnO	1.96	1.63	0.24	0.34	25.41	24.77
MnO	9.18	8.91	1.96	1.69	5.86	5.84
Sb$_2$O$_5$	0.00	0.00	0.00	0.00	0.15	0.00
MgO	28.09	27.66	24.79	25.26	1.21	1.40
CaO	1.10	0.87	12.02	12.46		
Na$_2$O	0.01	0.09	0.08	0.08		
K$_2$O	0.00	0.00	0.00	0.00		
Total	99.08	97.48	98.81	98.31	100.01	99.24
			formula proportions			
Si	7.93	7.98	8.00	7.90	0.003	0.000
Ti	0.00	0.00	0.00	0.00	0.000	0.001
Al	0.01	0.00	0.02	0.03	0.045	0.034
Fe^{3+}	0.03	0.03	0.01	0.01	1.950	1.967
Zn	0.20	0.17	0.02	0.03	0.733	0.719
Mn	1.05	1.04	0.22	0.19	0.194	0.195
Sb					0.002	0.000
Mg	5.68	5.66	4.97	5.11	0.071	0.082
Ca	0.16	0.13	1.73	1.81		
Na	0.00	0.03	0.02	0.02		
K	0.00	0.00	0.00	0.00		
Sum cations	15.06	15.02	15.00	15.10	2.997	2.998

Formulae based on 23 and 4 O atoms for amphibole and franklinite, respectively.

parentheses correspond to $T = 77$ K) are CS = 0.35 (0.44) mm/s, QS = 0.49 mm/s (0.51) and $\Gamma = 0.29$ (0.32) mm/s. The room-temperature values for CS and QS are typical of those normally found for $^{[6]}Fe^{3+}$ in oxides and hydroxides (McCammon 1995). The purpose of the experiment at 77 K was to test whether magnetic ordering occurs. None was found, but the asymmetry and line broadening encountered might be a next-nearest-neighbor effect that develops at this temperature (*i.e.*, we have more than one doublet).

X-RAY CRYSTALLOGRAPHY

Powder data

The powder X-ray-diffraction data presented in Table 4 were obtained using a Philips 1710 diffractometer with Cu anode and graphite monochromator. The data were collected at room temperature in the 2θ range 5–70°, the step width and counting time being 0.01° and 2.5 s, respectively. Peak positions were adjusted against an external silicon standard (SRM 640b). The unit-cell parameters of rinmanite (hexagonal cell), refined from twenty-seven reflections with the least-squares program of Novak & Colville (1989), are *a* 5.9889(4), *c* 9.353(1) Å, *V* 290.53(5) Å^3. The unit-cell parameter *a* of the associated franklinite was determined to be 8.451(1) Å.

Single-crystal data

The preliminary X-ray studies, carried out using image-plate techniques, showed that rinmanite has a hexagonal symmetry (dihexagonal-pyramidal class), space group $P6_3/mmc$, $P6_3mc$, or $P\bar{6}2c$. From the unit-cell dimensions obtained ($a \approx 6.0$, c ≈ 9.3 Å), we suspected that rinmanite is isostructural with the rare oxyhydroxide nolanite, (V, Fe, Ti, Al)$_{10}$O$_{14}$(OH)$_2$ (space group $P6_3mc$, *a* 5.89, *c* 9.26 Å; Hanson 1958, Gatehouse *et al.* 1983). Single-crystal X-ray data needed for a refinement of the structure were collected with a four-circle diffractometer (Siemens P4/RA) used with a rotating anode X-ray generator operated at 5.0 kW. The structural refinement was made using the SHELXTL PC software package (Sheldrick 1990), with neutral atomic scattering factors from the International Tables of Crystallography (Ibers & Hamilton 1974). Further experimental data are summarized in Table 5.

Crystal structure

As initial parameters for the structure refinement, we chose those of nolanite, taken from Gatehouse *et al.* (1983). The final result of the refinement procedure, with $R = 3.1\%$ for 199 unique diffraction intensities, confirmed the tentative structural model proposed for rinmanite and the space-group symmetry, $P6_3mc$. The atom positions and isotropic displacement parameters are given in Table 6, and selected bond-distances are given in Table 7. A table of structure factors is available from the Depository of Unpublished Data, CISTI, National Research Council, Ottawa, Ontario K1A 0S2, Canada.

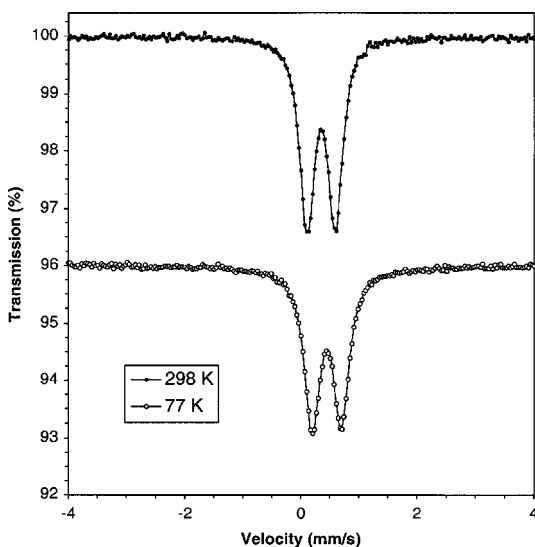Because of the relatively low number of observed independent reflections, a refinement where all non-

FIG. 4. Mössbauer spectra for rinmanite. For clarity, the curve for the spectrum at 77 K is displaced –4%.

TABLE 4. X-RAY POWDER-DIFFRACTION DATA FOR RINMANITE

$I(\%)$	d_{obs}(Å)	d_{calc}(Å)	h	k	l
20	5.187	5.187	1	0	0
17	4.539	4.536	1	0	1
34	3.474	3.473	1	0	2
43	2.994	2.994	1	1	0
44	2.673	2.672	1	0	3
12	2.593	2.593	2	0	0
100	2.522	2.522	1	1	2
20	2.499	2.499	2	0	1
2	2.338	2.338	0	0	4
10	2.267	2.268	2	0	2
8	1.9939	1.9937	2	0	3
2	1.9605	1.9603	1	2	0
2	1.9188	1.9186	1	2	1
2	1.8426	1.8430	1	1	4
13	1.8081	1.8079	2	1	2
7	1.7593	1.7597	1	0	5
8	1.7366	1.7366	2	0	4
4	1.7284	1.7288	0	3	0
28	1.6597	1.6595	2	1	3
15	1.6213	1.6216	3	0	2
2	1.5592	1.5589	0	0	6
33	1.5170	1.5171	2	0	5
54	1.4972	1.4972	2	2	0
2	1.4220	1.4218	1	3	1
3	1.3827	1.3827	1	1	6
5	1.3750	1.3749	3	1	2
8	1.3533	1.3533	2	1	5

TABLE 5. EXPERIMENTAL DETAILS OF THE CRYSTAL
STRUCTURE REFINEMENT OF RINMANITE

Refined formula	$Zn_2Sb_2Mg_{2.4(1)}Fe_{3.6(1)}O_{16}H_2$
Space group	$P6_3mc$
Unit-cell dimensions	$a = 5.993(1)$ Å
	$c = 9.335(2)$ Å
	$V = 290.36(9)$ Å^3
Formula units/unit cell	$Z = 1$
Density (calculated)	$5.13(1)$ g · cm^{-3}
Radiation	Mo$K\alpha$
Wavelength	0.71073 Å
Temperature	293(2) K
Intensity data collection	ω-2θ scan
Maximum sin(θ)/λ	0.8 Å^{-1}
Internal R	0.06
Collected reflections	1658
Unique reflections	199
Observed reflections	194
Criterion for significance	$I \geq 2\sigma$
Absorption correction	Numerical integration
Linear abs. coefficient	13.2 mm^{-1}
Transmission factor range	0.09–0.19
Structure refinement	Full matrix least squares
Minimized function	$\Sigma w \cdot (\Delta F^2)^{-1}$
Anisotropic thermal parameters	Zn and Sb
No. of refined parameters	21
Weighting scheme	$(\sigma^2 + 0.001 \cdot F^2)^{-1}$
R for observed reflections	0.030
wR for observed reflections	0.042
R for all unique reflections	0.031
Max. of $|\Delta|\sigma$	0.001
Max. and min. of $\Delta\rho$	1.6 and -2.2 e/Å^3

TABLE 6. ATOM COORDINATES FOR RINMANITE

Site	x	y	z	$U_{(eq)}$
M(1)*	0.1691(1)	-0.1691(1)	0.6862(4)	0.0289(11)
M(2)	1/3	2/3	0.3992(4)	0.0025(6)
M(3)	2/3	1/3	1/2	0.0047(13)
O(1)	0	0	0.0753(16)	0.001(3)
O(2)	1/3	2/3	0.7907(3)	0.026(6)
O(3)	0.1723(5)	-0.1723(5)	0.2872(12)	0.005(3)
O(4)	0.5209(4)	-0.5209(4)	0.0428(10)	0.0012(14)
H	0	0	-0.0067(5)	0.001(3)

* The refined site population of M(1) is 3.55(11) Fe + 2.45(11) Mg apfu.

hydrogen atoms are allowed to vibrate anisotropically would give an unacceptably low overdetermination ratio (observations:variables). To avoid an over interpretation of the data, it was therefore decided to keep the substitutionally disordered $M(1)$ atom as well as the oxygen atoms isotropic. The displacement parameter of the O(1) oxygen atom was kept identical to that of the attached hydrogen atom.

The $M(1)$ site is a mixed (disordered) Mg–Fe site. A refinement gave occupancy numbers of 0.41(2) for Mg and 0.59(2) for Fe, respectively. Site $M(2)$ contains only Sb, and Zn and the minor Mn content are assigned to $M(3)$. Bond-valence analysis (Brown & Altermatt 1985)

for the latter two sites yield empirical valences of +5.19 and +1.91 valence units, respectively, in good agreement with the formal charges of Sb^{5+} and Zn^{2+}. Full occupancy of all O sites is indicated. The location of H was determined from a minor electron-density peak in the difference-Fourier map centered about (0, 0, 0); this position was earlier postulated as the H site from valence-sum calculations of the nolanite structure (Gatehouse *et al.* 1983). The refined O–H distance, 0.8(1) Å, compares well with typical bond-lengths observed in other structures (*e.g.,* goethite with 0.88 Å; Szytuta *et al.* 1968).

The unit cell of rinmanite ideally thus contains one formula unit of $Zn_2Sb_2[Mg_2Fe_4]O_{14}(OH)_2$. The basic arrangement of atoms is that of the hexagonal $M_2Mo_3O_8$ compounds, which include the mineral kamiokite, $Fe_2Mo_3O_8$ (McCarroll *et al.* 1957, Kanazawa & Sasaki 1986). In that structure, the cations occupy voids of a hexagonal closest-packed framework of O atoms in layers stacked along [0001], with Mo atoms in octahedral co-ordination and M^{2+} atoms equally distributed over octahedral and tetrahedral sites. Adopting the site labels as used for nolanite, the $M(1)$ octahedra in rinmanite form a layer by sharing edges; a parallel second layer is formed by corner-sharing between the $M(2)$ octahedra and the $M(3)$ tetrahedra (Figs. 5, 6). Also belonging to the mixed layer are structural voids, which are unoccupied in the molybdate compounds, but contain the hydrogen atoms in rinmanite.

DISCUSSION

The intracrystalline distribution of cations in nolanite could not be determined unambiguously by Gatehouse *et al.* (1983), mainly because of the small differences in the scattering factors among the elements involved and the many possible choices of valence states. The model described here for rinmanite is quite straightforward in comparison. In terms of average bond-lengths, the most striking difference between the two minerals is found in

TABLE 7. SELECTED BOND DISTANCES
(Å) FOR RINMANITE AND NOLANITE

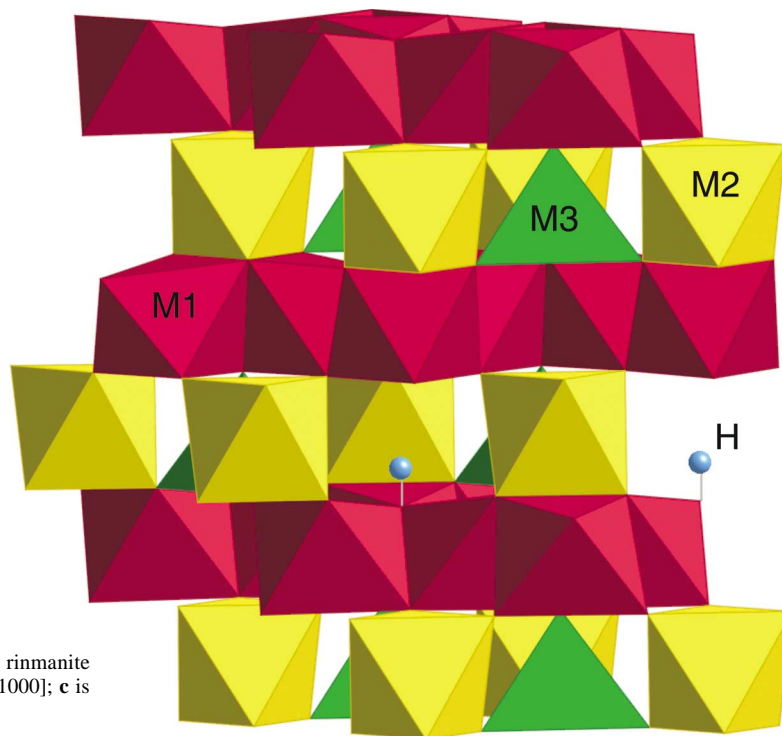|		rinmanite	nolanite
M(1)–O(2)		1.964(12)	2.015(3)
M(1)–O(3)	×2	2.008(6)	1.951(3)
M(1)–O(1)		2.038(8)	2.043(2)
M(1)–O(4)	×2	2.100(8)	2.040(4)
<M(1)–O>		2.036	2.007
M(2)–O(3)	×3	1.971(7)	1.965(4)
M(2)–O(4)	×3	2.022(7)	2.083(3)
<M(2)–O>		1.996	2.024
M(3)–O(2)		1.953(24)	1.905(6)
M(3)–O(4)	×3	1.987(3)	1.928(3)
<M(3)–O>		1.978	1.922
O(1)–H		0.77(17)	

FIG. 5. The crystal structure of rinmanite viewed approximately along [1000]; **c** is vertical in the drawing.
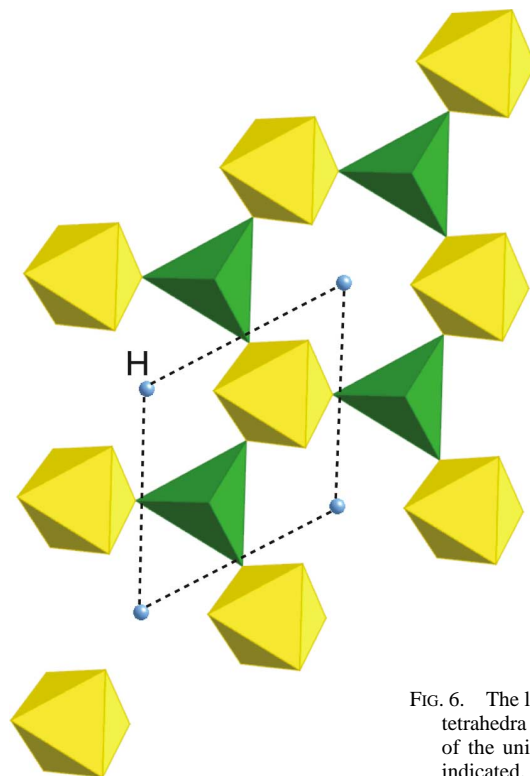

FIG. 6. The layer of corner-sharing $M(2)$ octahedra and $M(3)$ tetrahedra at $z \approx 0.5$ in the structure of rinmanite. The origin of the unit cell is at the position of the hydrogen atom indicated.

the bond lengths involving the $M(3)$ site (Table 7). This is in agreement with the assignment of a fraction of Fe^{3+} to this site in nolanite. Gatehouse *et al.* (1983) furthermore proposed that Ti^{4+} occupies $M(1)$ in nolanite; in view of the present results and considering the similarity in charge and ionic size between Ti^{4+} and Sb^{5+}, $M(2)$ might be a better suggestion.

In the detailed description of nolanite, Gatehouse *et al.* (1983) addressed the question whether the mineral is stoichiometric with respect to the H content or not. If we assume a constant O content of 16 atoms per formula unit (*apfu*) for rinmanite, and taking the average wt.% oxide value in Table 2, 1.99 H *apfu* are required to obtain charge balance. There is, however, an antipathetic relation between Mg and Fe (Fig. 7A) if all analytical points are considered (linear correlation coefficient $r = -0.70$). To explain this variation and to preserve electroneutrality, a coupled ionic substitution of the type $Mg^{2+} + H^+ = Fe^{3+} + \square$ would seem to be necessary. In addition to this, there is a negative correlation ($r = -0.73$) between Mg and (Zn + Mn), which suggests that in situations where Mg > 2 *apfu*, the excess amount of this cation enters the $M(3)$ tetrahedra (Fig. 7B).

Nolanite and rinmanite are compositionally dissimilar, but in view of their isostructural relationship, they constitute a new mineral group within the oxide–hydroxide class. Other closely related minerals, on the basis of close-packed anion frameworks of (O + OH), are nigerite (Grey & Gatehouse 1979) and members of the högbomite group (Armbruster 1998); they contain nolanite-like layers in their atomic structures.

From the textural observations, it is clear that rinmanite has largely grown after franklinite, but there is no indication of replacement. As both phases are based on closest-packed arrays of O atoms, an orientation relationship with [111] of the spinel parallel with [0001] of rinmanite seems probable (but is not yet confirmed); this would give a lattice misfit (based on the cell parameters given above) of less than 0.4%. The presence of franklinite might then promote the nucleation of rinmanite. Interestingly, epitaxy also seems to be possible between rinmanite and coexisting talc; the 002 interplanar spacing of talc, ($c \cdot \sin \beta$)/2 = 9.35 Å, is equal to the c-axis repeat of rinmanite. Both minerals clearly have layer structures, but no simple mechanism of growth can be formulated at present.

The amphibole + talc assemblage is interpreted to be a product of regional metamorphism of a siliceous dolomite (alternatively, talc may have formed by retrograde replacement of tremolite, but this is not supported by textural observations). The question of interest here is whether the oxide subsystem, which contains nearly all of the metals Sb, Fe, and Zn in the paragenesis, has formed as a result of thermal breakdown of sulfide precursors or whether it represents an original high-$f(O_2)$ environment in the protolith. A third alternative would be that the key elements have been introduced from
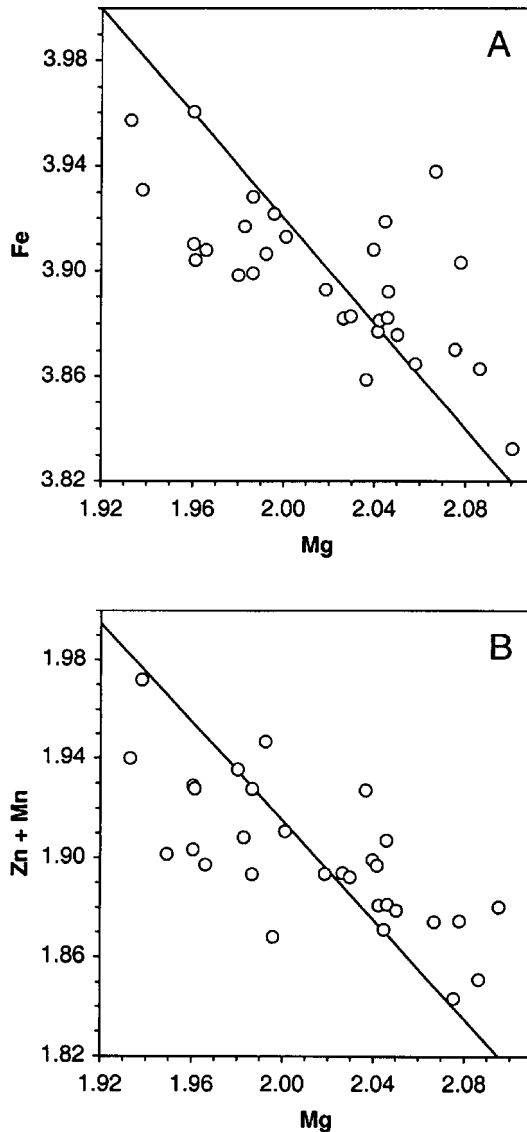

FIG. 7. A. Plot of Mg *versus* Fe calculated for 10 metal atoms per unit cell in rinmanite. B. Mg *versus* (Zn + Mn). The slope of the lines (merely serving as a guide for the eye) is –1.

sulfide-rich zones by synmetamorphic metasomatism. Although the formation of gahnite at the expense of sphalerite, for example, is well documented from metamorphosed massive sulfide deposits (*e.g.,* Zaleski *et al.* 1991), it seems unrealistic to propose that desulfidation and oxidation have occurred to such a complete extent in a restricted zone. Rather, the effects of metamorphism on sulfide assemblages at Garpenberg Norra seem to be

limited to annealing and deformation (Sandecki 1983). With the small amount of data at hand, we find it more plausible that the association franklinite–rinmanite is essentially a product of metamorphism of syndepositional constituents, under the influence of an aqueous fluid that favored the formation of hydroxyl-bearing phases like amphibole, talc and rinmanite. The association of Zn–Sb–As–Ba oxyminerals is of course rare, but largely reminiscent of assemblages found in the Långban-type Mn–Fe deposits (Holtstam *et al.* 1998), situated in similar, contemporaneous host-rocks some 120 km southwest of the Garpenberg ore field.

REFERENCES

ALLEN, R.L., LUNDSTRÖM, I., RIPA, M., SIMEONOV, A. & CHRISTOFFERSON, H. (1996): Facies analysis of a 1.9 Ga, continental margin, back-arc, felsic caldera province with diverse Zn-Pb-Ag-(Cu-Au) sulphide and Fe oxide deposits, Bergslagen region, Sweden. *Econ. Geol.* **91**, 979-1008.

ARMBRUSTER, T. (1998): Zincohögbomite-8*H* from Samos (Greece): crystal structure, polysomatism, and polytypism in högbomite related structures. *Schweiz. Mineral. Petrogr. Mitt.* **78**, 461-468.

BROWN, I.D. & ALTERMATT, D. (1985): Bond-valence parameters obtained from a systematic analysis of the inorganic crystal structure database. *Acta Crystallogr.* **B41**, 244-247.

CRIDDLE, A.J. & STANLEY, C.J. (1993): *Quantitative Data File for Ore Minerals* (3rd ed.). Chapman and Hall, London, U.K.

GATEHOUSE, B.M., GREY, I.E. & NICKEL, E.H. (1983): The crystal chemistry of nolanite, (V,Fe,Ti,Al)$_{10}$O$_{14}$(OH)$_2$, from Kalgoorlie, Western Australia. *Am. Mineral.* **68**, 833-839.

GREY, I.E. & GATEHOUSE, B.M. (1979): The crystal structure of nigerite-24*R*. *Am. Mineral.* **64**, 1255-1264.

HANSON, A.W. (1958): The crystal structure of nolanite. *Acta Crystallogr.* **11**, 703-709.

HOLTSTAM, D., NYSTEN, P. & GATEDAL, K. (1998): Parageneses and compositional variations of Sb oxyminerals from Långban-type deposits in Värmland, Sweden. *Mineral. Mag.* **62**, 395-407.

IBERS, J.A. & HAMILTON, W.S., eds. (1974): *International Tables for X-Ray Crystallography* **IV**. Kynoch Press, Birmingham, U.K.

JERNBERG, P. & SUNDQVIST, T. (1983): A versatile Mössbauer analysis program. *Univ. of Uppsala, Inst. of Physics, Rep.* **UUIP-1090**.

KANAZAWA, Y. & SASAKI, A. (1986): Structure of kamiokite. *Acta Crystallogr.* **C42**, 9-11.

MANDARINO, J.A. (1981): The Gladstone–Dale relationship. IV. The compatibility concept and its application. *Can. Mineral.* **19**, 441-450.

MCCAMMON, C. (1995): Mössbauer spectroscopy of minerals. *In* Mineral Physics & Crystallography: a Handbook of Physical Constants (T.J. Ahrens, ed.). American Geophysical Union, Washington, D.C. (332-347).

MCCARROLL, W.H., KATZ, L. & WARD, R. (1957): Some ternary oxides of tetravalent molybdenum. *J. Am. Chem. Soc.* **79**, 5410-5414.

NOVAK, G.A. & COLVILLE, A.A. (1989): A practical interactive least-squares cell-parameter program using an electronic spreadsheet and a personal computer. *Am. Mineral.* **74**, 488-490.

POUCHOU, J.-L. & PICHOIR, F. (1991): Quantitative analysis of homogeneous or stratified microvolumes applying the model "PAP". *In* Electron Probe Quantitation (K.F.J. Heinrich & D.E. Newbury, eds.). Plenum Press, New York, N.Y. (31-75).

SANDECKI, J. (1983): A textural study of pyrite, sphalerite and galena from Garpenberg Norra, south central Sweden. *Geol. Fören. Stockholm Förh.* **105**, 213-222.

SHELDRICK, G.M. (1990): *SHELXTL, a Crystallographic Computing Package* (version 4.1). Siemens Analytical X-ray Instruments, Inc., Madison, Wisconsin.

SZYTUTA, A., BUREWICZ, A., DIMITRIJEVIĆ, Ž., KRAŚNICKI, S., RŻANY, H., TODOROVIĆ, J., WANIC, A. & WOLSKI, W. (1968): Neutron diffraction studies of α-FeOOH. *Phys. Stat. Solidi* **26**, 429-434.

VIVALLO, W. (1984): The metamorphism of the supracrustal rocks at Garpenberg, south central Sweden. *Geol. Fören. Stockholm Förh.* **106**, 257-267.

_____ (1985): The geology and genesis of the Proterozoic massive sulfide deposit at Garpenberg, central Sweden. *Econ. Geol.* **80**, 17-32.

ZALESKI, E., FROESE, E. & GORDON, T.M. (1991): Metamorphic petrology of Fe–Zn–Mg–Al alteration at the Linda volcanogenic massive sulfide deposit, Snow Lake, Manitoba. *Can. Mineral.* **29**, 995-1017.